catalysts

MDPI

Article

Application of Biochar from Woodchip as Catalyst Support for Biodiesel Production

Nor Shafinaz Azman [1], Nozieana Khairuddin [1,2,*], Tengku Sharifah Marliza Tengku Azmi [1], Sivasangar Seenivasagam [1,2] and Mohd Ali Hassan [3]

[1] Department of Science and Technology, Faculty of Humanities, Management and Science, Universiti Putra Malaysia Bintulu Sarawak Campus, Bintulu 97008, Malaysia
[2] Institut Ekosains Borneo, Universiti Putra Malaysia Bintulu Sarawak Campus, Bintulu 97008, Malaysia
[3] Department of Bioprocess Technology, Faculty of Biotechnology and Biomolecular Sciences, Serdang 43400, Malaysia
* Correspondence: nozieana@upm.edu.my; Tel.: +60-86-855823

Abstract: In Asian countries, the primary palm oil producers, used cooking oil (UCO) is the primary feedstock for biodiesel production. It can be converted into an eco-fuel for application in heavy machinery and diesel engine vehicles due to its low carbon emissions and low global warming potential. However, the illegal dumping of UCO containing triglyceride into flowing water bodies (resulting in wastewater treatment and purification complications) has prompted the design of smart UCO collection systems. This study aims to investigate the heterogeneous catalytic performance of biochar as a support catalyst derived from woodchips calcined at 400 °C and 800 °C under nitrogen gas flow. The catalyst was synthesized through the wet impregnation method using two metal oxides (5 wt.%, nickel and molybdenum) via transesterification to enhance the biodiesel yield. High biodiesel yield was obtained through the controlled parameters: 65–95 °C temperature, 10:1 methanol to oil ratio, and 2 h reaction time. The synthesized catalyst was characterized through X-ray Diffraction (XRD) and Field Emission Scanning Electron (FESEM). The biodiesel production was confirmed by Fourier Transform Infra-Red (FTIR) Spectroscopy. The results showed that the highest biodiesel yield was produced by the catalyst calcined at 800 °C, which shows a consistent trend in the yields obtained at temperatures in the order 75–85–95–65 °C. In conclusion, calcination at 800 °C resulted in a higher yield (74.66%) and catalyst reusability (≥5 cycles).

Keywords: used cooking oil; biodiesel; biochar; woodchips; heterogenous catalysis; wet impregnation; transesterification

check for updates

Citation: Azman, N.S.; Khairuddin, N.; Tengku Azmi, T.S.M.; Seenivasagam, S.; Hassan, M.A. Application of Biochar from Woodchip as Catalyst Support for Biodiesel Production. *Catalysts* **2023**, *13*, 489. https://doi.org/10.3390/catal13030489

Academic Editor: Anastasia Macario

Received: 3 August 2022
Accepted: 17 September 2022
Published: 28 February 2023

Copyright: © 2023 by the authors. Licensee MDPI, Basel, Switzerland. This article is an open access article distributed under the terms and conditions of the Creative Commons Attribution (CC BY) license (https://creativecommons.org/licenses/by/4.0/).

1. Introduction

The rapid growth in the human population is linked to increased energy demand, especially in the development of the industrial and transportation sectors. This observation is due to humanity's overdependence on nature's fast depleting resources such as petroleum, natural gas, and coal. Alternative fuels such as biodiesel are under consideration as a replacement for these non-renewable energy resources [1]. According to [2], lipid-rich renewable feedstocks (e.g., animal fats, vegetable oil, and algae-derived mixtures of fatty acid methyl esters) can be converted into bioethanol and biodiesel. One of the most notable outcomes of biodiesel in terms of substituting fossil fuels is good engine performance [3]. According to [2] the presence of excess monoglycerides and free fatty acid compounds enhance biodiesel lubrication properties, while low sulphur content guarantees biodegradability and environmental friendly properties.

A recent study [3] reported that a continuous supply of feedstock sources is crucial for energy security, and sustainable economic development supports these findings. As reported in [4,5], energy sources are required to fulfil the needs of various industries that

currently depend on expensive gasoline and non-renewable energy resources [6]. Furthermore, the combustion of conventional fossil fuels and non-renewable resources generate significant toxic gases, which harm the environment. Thus, researchers worldwide are aiming to develop alternative green energy systems, production processes, and quality products that not only have similar properties to conventional fuel but also minimize/eliminate fossil fuel dependency [6].

For example, biodiesel or Fatty Acid Methyl Ester (FAME) is a well-known biofuel that is substitutable for crude oil-derived gasoline. FAME consists of highly oxygenated molecules, which has drawbacks including high viscosity, poor cloud and pour points, low heating value, and low oxidation stability [7]. The transesterification process remains the most common approach for biodiesel synthesis [8]. According to this method, an optimal methanol ratio is needed for the optimal reaction between the vegetable oil (or fat) feedstock and alcohol, with or without a catalyst to produce high FAME yield through triglyceride conversion to di- and mono-glycerides. The three-step reversible reaction generates di- and mono-glycerides as intermediate products.

Currently, the synthesis of heterogeneous catalysts for enhancing biodiesel production is trending due to its low production costs, reusability, and stability, even under extreme reaction conditions. Post reactions also promise less water consumption and easy separation of biodiesel and glycerol [9], while simultaneous transesterification reactions can occur, thereby ensuring efficiency. In contrast, other studies [10] have demonstrated the emergence of three phases (solid-alcohol-oil) and mass transfer constraints during transesterification using solid catalysts. Basic or acid solid catalysts can be used to accelerate the transesterification reaction. K, Na, Ca, or Mg oxides supported on Al_2O_3, basic zeolites, and other essential materials are the most extensively used heterogeneous base catalysts.

To produce a high output of biodiesel, these catalysts must be used in large quantities. Strong acidic ion exchange resins (e.g., amberlyst), acid zeolites, and sulfated zirconia have also been reported as heterogeneous solid acid catalysts. However, this class of catalysts are not only expensive but also have low intrinsic activity. Alternatively, the utilization of biomass waste in the form of biochar as a catalyst support is an interesting catalytic approach. A carbon-based catalyst made from biomass is both a green and waste-to-energy technology. The pyrolysis process produces a carbon-rich catalyst, and the residue is known as biochar. This biochar works well as a biocatalyst in the production of biodiesel. Palm seed, rice husk, groundnut shell, date seeds, seaweeds, and other waste biomass are used to make biochar [11]. In a study reported by [12,13] utilized biochar obtained from avocado under pyrolysis were synthesized and doped with several nanostructured calcium oxides which were then deposited onto the biochar and then underwent transesterification to produce biodiesel. Application of these biochars showed a relatively high porosity and an alveolar surface, whose pore size are capable of allocating and anchoring different metallic active species.

In the past, deoxygenation (DO) processes have been studied using various catalysts, including Pd- and Pt-based transition metal oxides such as Ni, Co, Zn, Cu, Ga, and Ru [14,15]. The formation of acidity-basicity characteristics by the desegregation of a nanosized CaO–a_2O_3/AC catalyst on a carbon support has previously been shown to be useful for biodiesel production [16]. The use of a bimetallic acid oxide NiO–MoO/AC catalyst on a DO reaction at 350 °C with a run-time of 3 h achieved biodiesel yield below 35% and n-(C_8–C_{20}) hydrocarbon fractions in the range 89.93–82.81%. In the current study, the synthesized catalyst will be conducted in a transesterification process to investigate the catalytic potential and biodiesel yield obtained for up to five times reusability.

Another potential area for research is nanoscale materials. The catalytic characteristics of mixed metal oxides are determined mainly by their microstructure. The surface to volume ratio increases significantly in the nanoparticle phase, and the surface atoms encompass an increasing fraction of the total particulate volume with high defect patterns [17]. As a result, they may display intriguing, new, or improved chemical process properties. In this study, nanocrystalline NiMoO4 was synthesized and incorporated onto biochar

from a woodchip with a particle size of 20 nm observed through FESEM. The ability of the catalysts and the biodiesel yield were examined based on the procedure reported in the literature [18].

Therefore, this research seeks to analyse the catalytic synthesis potential applied to the transesterification reaction, and the breakdown performance of hydrocarbon chains. The paper will provide valuable information regarding the overall process of UCO transesterification using a synthesized catalyst. Thus, process intensification in the clean energy industry will overcome the economic issues related to the rising prices and depleting supplies of conventional fuels sources.

2. Results and Discussion

2.1. Acid Value and Free-Fatty Acid (FFA%) Content of UCO

Table 1 below shows the calculated acid value of UCO. As observed, the acid value of UCO was below 7.6 mg KOH/g, which necessitated direct single step transesterification to produce biodiesel [19]. This means there was no need for the UCO to undergo pre-treatment or acid esterification.

Table 1. FFA content for UCO.

No. of Replicates	Acid Value	FFA	Biodiesel
1	±5.230	±2.615	±1.0727
2	±4.265	±2.133	±0.6926
3	±5.905	±2.953	±1.0595
Average	±5.133	±2.567	±0.9416

2.2. Biodiesel Yield over Reaction Temperature

The results of the catalytic reactions of the woodchip (BWC/NiO–MoO400 and BWC/NiO–MoO800) catalysts are shown in Figure 1. For transesterification using BWC/NiO–MoO400 catalyst, the UCO yield was the highest at 76.66% for a reaction temperature of 75 °C; however, the UCO yield was lower at higher reaction temperatures. In contrast, BWC/NiO–MoO800 shows the highest UCO yield of 74.66% at 75 °C at higher temperatures. The study by [20] confirmed that higher reaction temperatures i.e., above the optimal values, do not to increase biodiesel yield.

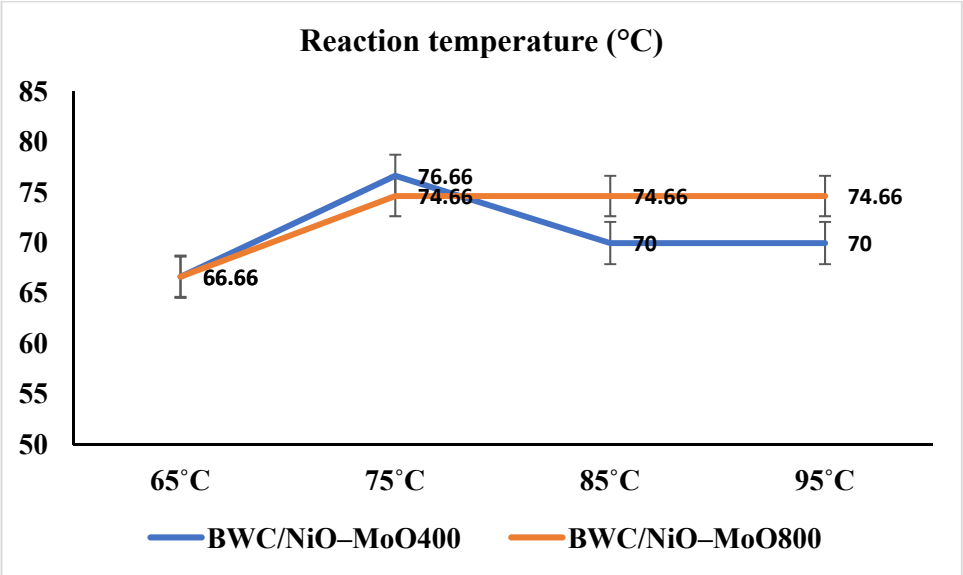


Figure 1. Biodiesel yield (%) obtained at various reaction temperatures (°C) of biochar woodchip.

The feedstock is helped to cross the activation energy barrier by increased temperature [21] (Hanif et al., 2018). Due to the agitation speed, the reaction mixture is treated as a pseudo-homogeneous system with uniform composition and no mass transfer constraint, allowing for chemical control of the kinetics of the entire process [22]. When the concentration of one reactant (Methanol) is greater than the concentration of the other reactant (Triglyceride), the second order reaction becomes a pseudo-order reaction [23]. The irreversible pseudo-first order triglyceride conversion rate by methanolysis can be expressed using these principles.

2.3. Catalyst Reusability Performance over UCO Biodiesel Yield

The reusability of biochar woodchip catalysts (BWC/NiO–MoO400 and BWC/NiO-MoO800) after the transesterification of UCO is shown in Figure 2. The fixed parameters were: 5 wt.% catalyst concentration, 1:10 UCO to methanol molar ratio, 60 min reaction time, and different reaction temperatures ranging from 65–95 °C. The transesterification process using the different calcined temperature catalysts was carried out repeatedly for five cycles. Figure 3 shows the UCO yield for each cycle of transesterification using woodchip (BWC/NiO–MoO800 and BWC/NiO–MoO400). For the BWC/NiO–MoO800 catalysts, the yield on the first cycle was 66.66% but slightly increased to 74.66% on the second and third reactions consistently, before slight increasing to 83.33% in the fifth cycle.

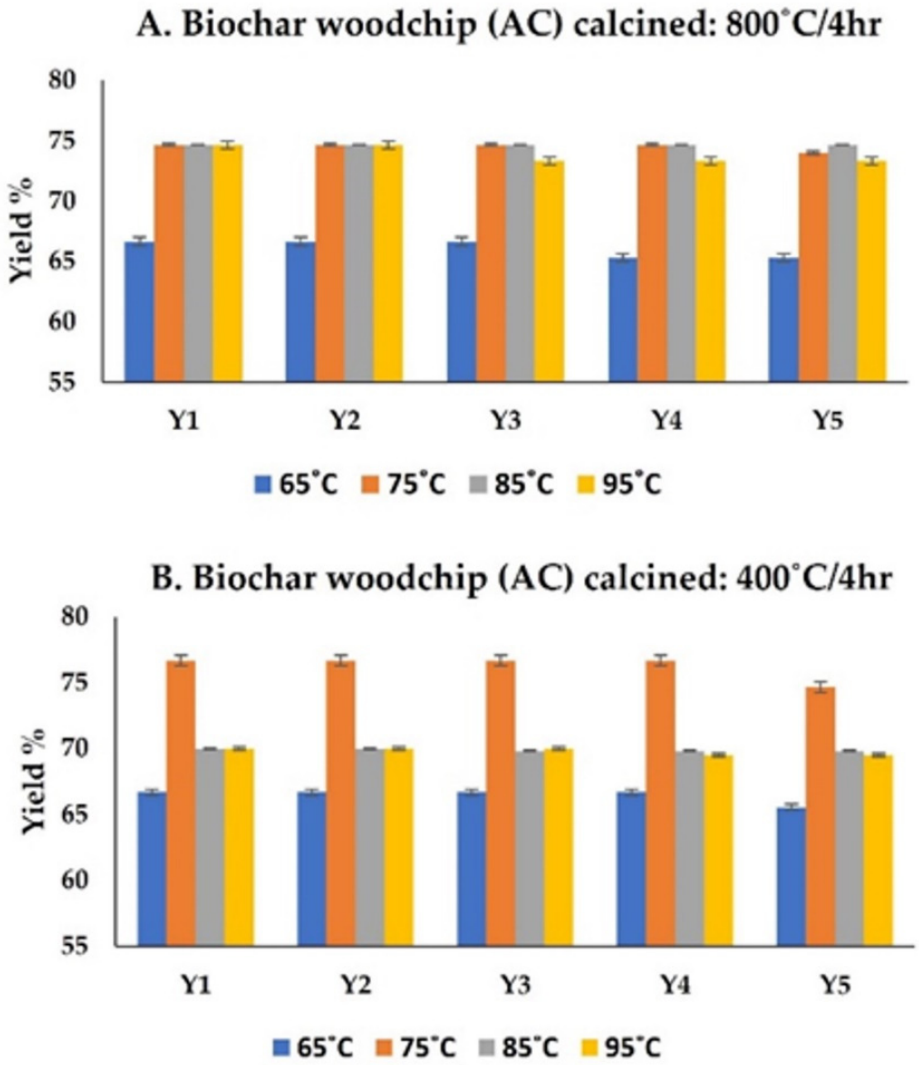


Figure 2. Catalyst reusability performance over reaction temperature. (**A**) 800 °C; (**B**) 400 °C.

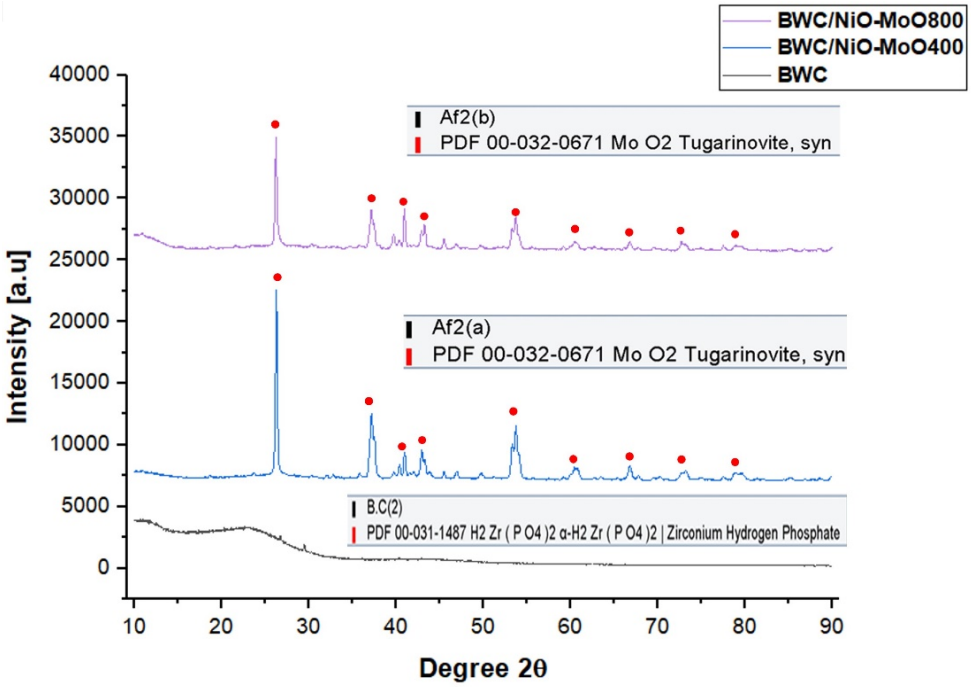


Figure 3. XRD diffraction of before and after calcined woodchip biochar catalyst incorporated with NiO-MoO/BWC.

The BWC/NiO–MoO400 showed a moderate yield of 66.66% in the first reaction. The yield trend gradually reduced from the second cycle to the fifth cycle. The reduced yield obtained from the group catalyst calcined under 800 °C (BWC/NiO–MoO800) was ~10%. In contrast, the catalyst calcined under 400 °C (BWC/NiO–MoO400) was ~18%. The low biodiesel yield after the fourth cycle was caused by the loss of active catalytic sites. The lost catalytic sites may have been due to structural changes in the catalyst's surface morphology [24]. The catalyst's surface changed after repeated calcination or sintering [25]. Another reason for the reduction of UCO yield is the leaching of metal ions into the biodiesel, which causes saponification [26,27] Using rice-husk solid acid biochar in the temperature range 70–110 °C obtained higher biodiesel yield.

2.4. Characterization of Catalysts

2.4.1. Diffraction of X-rays (XRD)

The sharpest peak observed for the woodchip biochar is 26,0° at 2θ. The higher the crystallinity degree of the fibrous-like structure, the sharper the diffraction peak. The XRD pattern of the woodchip biochar calcined at 400 °C and 800 °C for 4 h and fresh woodchip biochar is shown in Figure 3. The XRD peak distance in the adjacent graph is attributed to high crystallinity which is a clear hallmark of nickel and molybdenum metal integration. Based on the graph, there is a significant difference in the chemical composition in woodchip biochar before and after calcination (Figure 3). The data analysis revealed intense MoO_2 peaks with different classifications of molybdenum states visible for all samples. The states represent molybdenum tugarinovite (BWC/NiO-MoO800) at (2θ = 26.00°, 31.50°, 37.30°, 41.50°, 49.50°, 54.00°, 60.00°, 66.50°, and 78.00°]). Whilst, for BWC/NiO-MoO400 the peak was observed at (2θ = 26.00°, 31.50°, 37.00°, 42.00°, 49.00°, 54.00°, 60.00°, 66.50°, 72.00° and 78.00° (PDF card no: 00-032-0671)) as shown in Figure 4.

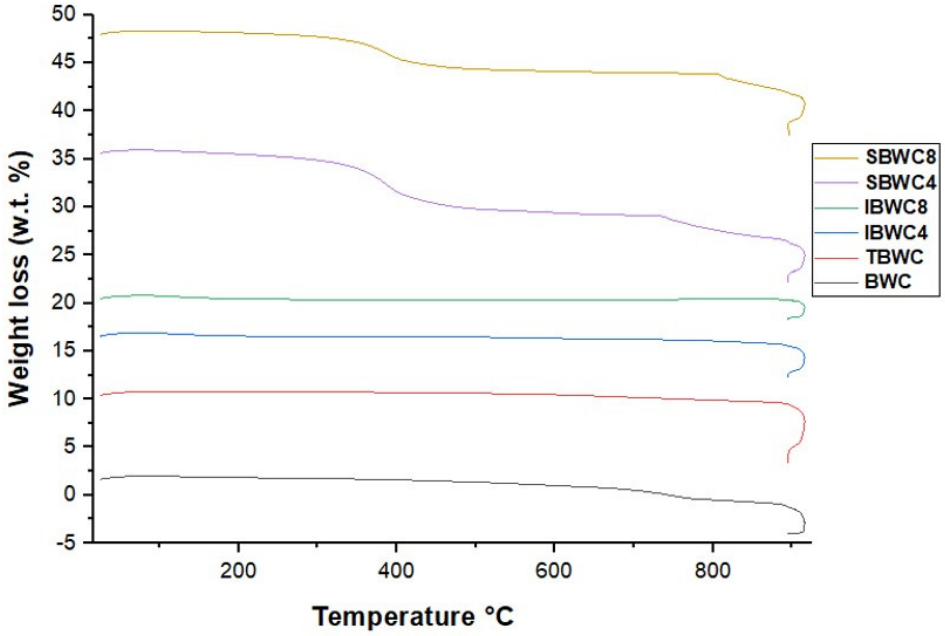


Figure 4. Thermal gravimetry decomposition of prepared catalyst from biochar woodchip.

2.4.2. Thermal Degradation Study of the Biochar Catalyst Using Thermogravimetric Analysis (TGA)

As shown in Figure 4, lignin did not show a well-defined degradation peak. On the contrary, the degradation process started at 100 °C and continued gradually up to 800 °C, a temperature at which more than 80 wt.% of the initial mass had been decomposed [28], corresponding to approximately 15 wt.% of the total weight of the raw material. As can be seen in the TGA, a large part of the weight loss had already occurred in BWC at 748 °C which indicated that the sample consisted mainly of water, lignin, cellulose, and hemicellulose. The significant thermal degradation of BWC started at 748 °C and continued gradually up to 890 °C which was a loss of about 83 wt.% of the initial mass. Finally, at 800 °C, there was still less than about 10 wt.% of fresh biochar undegraded by pyrolysis, which corresponds to the carbon and metallic residues.

Significant thermal degradation of BWC/NiO–MoO400 was detected at 800 °C and it continued its initial loss up to 70 wt.% by 880–920 °C. Whereas the degradation process of BWC/NiO–MoO800 started at 680 °C and continued gradually up to 890 °C, which was a loss of about 83 wt.% of the initial mass. The calcined catalyst in 800 °C showed faster coke decomposition than 400 °C, due to the wider surface area of catalyst with the aid of high reactivity of metal incorporated on it. The population of the acid site has a significant impact on the catalyst's activity, according to the study conducted by [29], which confirmed that strong transesterification activity was accompanied by a low specific surface area when the acid density was comparable. However, a large specific surface area and high acid density led to high biodiesel yield.

Significant thermal degradation of set SA and SB (BWC) were detected at 380 °C and continued to reduce its initial loss up to 50 wt. The spent catalyst performance and stability at high temperatures up to 900 °C decreased almost 50% after five cycles. This corresponded to the analysis of the catalyst before the reaction where it was associated with the combustion of the nanorod bulk of AC [18]. The spent catalyst showed a rapid loss from its original weight due to its decomposition temperature (700 °C), which indicates indicative of the oxidation of coke in the air.

2.4.3. Field Emission Scanning Electron Microscope (FESEM)

The FESEM micrographs of the catalyst and CaO produced from the woodchip biochar are shown in Figure 5. The morphology of CaO, which was isolated using acid pre-

treatment under reflux and subsequently purified, is also shown in Figure 5. The typical drying procedure that utilises universal oven heating at 100 °C transformed the treated biochar morphology into solid crack with a plate-like structure (Figure 6A,B). The morphology of the catalyst, as seen in the figure, showed no aggregation of biochar with the indicated transition metal. However, during the wet impregnation procedure the particles were well scattered.

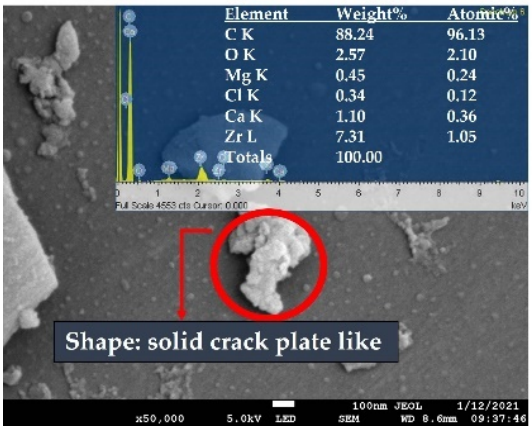


Figure 5. Surface morphology of woodchip biochar before calcination.

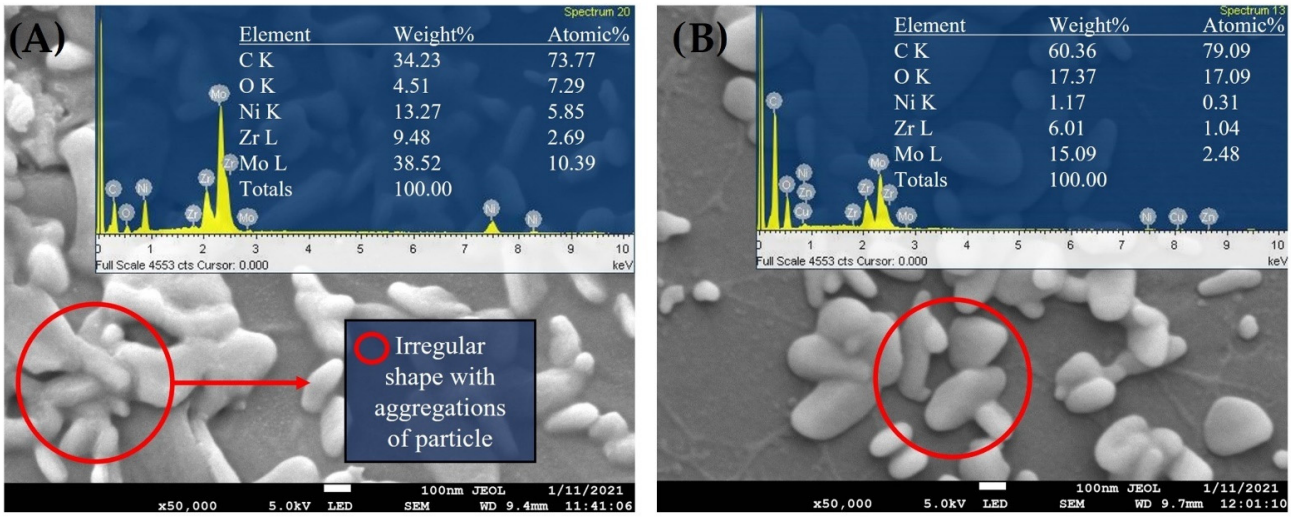


Figure 6. FESEM images of impregnated Biochar AC with metal oxide at (**A**) 400 °C and (**B**) 800 °C.

Figure 7A,B shows the crystallites of cellulose that formed a rod-like shape in the study conducted by [30] which were observed in its morphology investigations. The surface morphology of the biochar before and after calcination (calcined at 400 °C and 800 °C, respectively, in 4 h under N_2 gas flow) is shown. The figure suggests a poor particle surface area due to the large particle size and irregularly shaped aggregates of carbon. In comparison to raw biochar, the morphological features of calcined biochar have changed, resulting in particles with smaller particle- and agglomerate-sizes. A similar spherical shape, morphology, and structure for CaO obtained from the calcination treatment of eggshells has been reported in the literature [31]. Smaller particles could have a larger specific surface area. The surface area of the catalyst increases as the particle size decreases, which increases the active sites and the reaction rates. Consequently, the catalyst's active sites reacted equally during the transesterification reaction. These modifications were caused by hydrogen bond fractures in the crystalline region caused by acid treatment, which triggered the creation of a nanocrystalline fibrous-like structural pattern on the surface of activated charcoal [32]. The addition of the NiO–MoO/BWC bimetallic phase

caused particle expansion, as expected from the combination of intercalated metals (NiO and MoO) during synthesis.

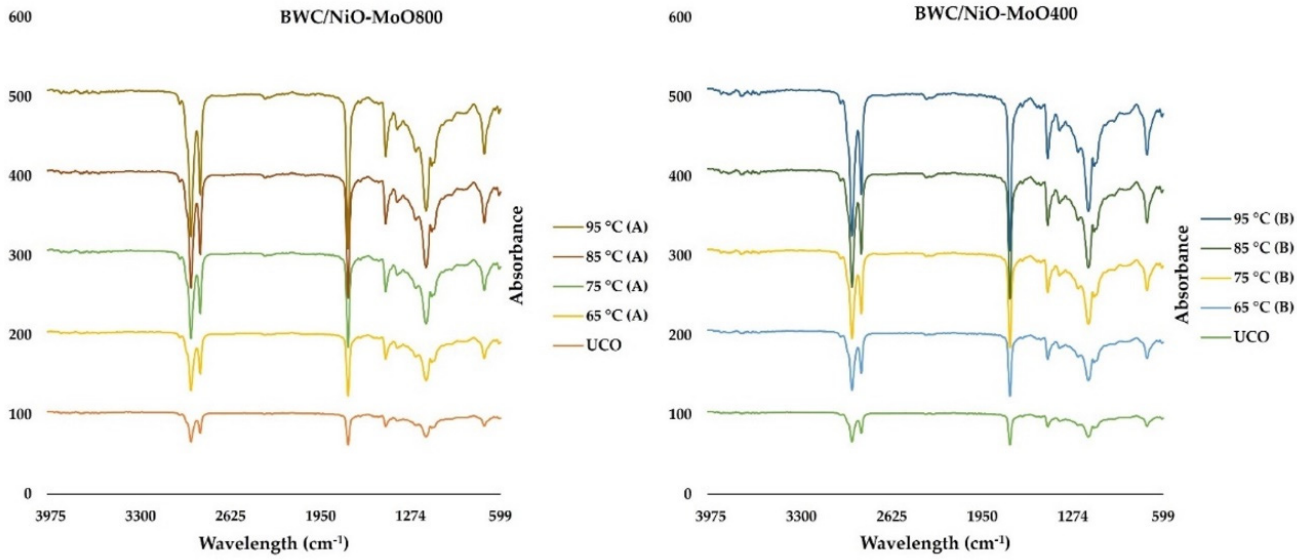


Figure 7. Chemical functional groups of triglycerides and transesterified products at (**A**) 800 °C and (**B**) 400 °C under FTIR analysis.

2.5. Characterization of UCO Biodiesel

2.5.1. Fourier Transform Infrared (FTIR) Spectroscopy

Based on this experiment, the chemical functional groups of the triglycerides and transesterified products were analyzed. The spectrum in Figure 7 shows that C–H stretching bands can be observed in the region between 3000 cm^{-1} and 2800 cm^{-1} on all spectra of UCO and biodiesel. Strong absorption peaks can be observed at 1743.65 $cm^{-1}$and 1739.79 cm^{-1} on UCO and BUCO spectra, respectively. These peaks correspond to the presence of the C=O group [33]. The peaks observed at 1456 cm^{-1} for the UCO spectrum and 1450.47 cm^{-1} for the biodiesel spectrum are the result of the methylene group $–CH_2$ bending. The presence of the C–O group of esters can be attributed to peaks at 1157.29 cm^{-1} and 1168.86 cm^{-1} for the UCO and biodiesel spectra, respectively. The noticeable bands at 719.45 cm^{-1} on the UCO and biodiesel spectra correspond to the alkene C=C group [34].

2.5.2. Fatty Acid Compound Detection by Gas Chromatography-Mass Spectrometry

A higher ester amount indicates good quality biodiesel formation with lower amounts of side products. Usually the purpose of the GC-MS analysis is to determine the mass of the fragmented compound and increase the ease of detecting isomers in accordance with the National Institute of Standards. However, the different result for hydrocarbon in the range of n-(C8–C20) obtained from GC-MS, clearly proved that mostly straight chain hydrocarbons (saturated and un-saturated) were found in the transesterified liquid product. Only a small amount of heavy C21–C24 hydrocarbons and oxygenated intermediates were detected, such as ketones, aldehydes, alcohol, and carboxylic acid. Various fatty acid compounds and their corresponding peaks identified from GC-MS are provided in Figure 8 below.

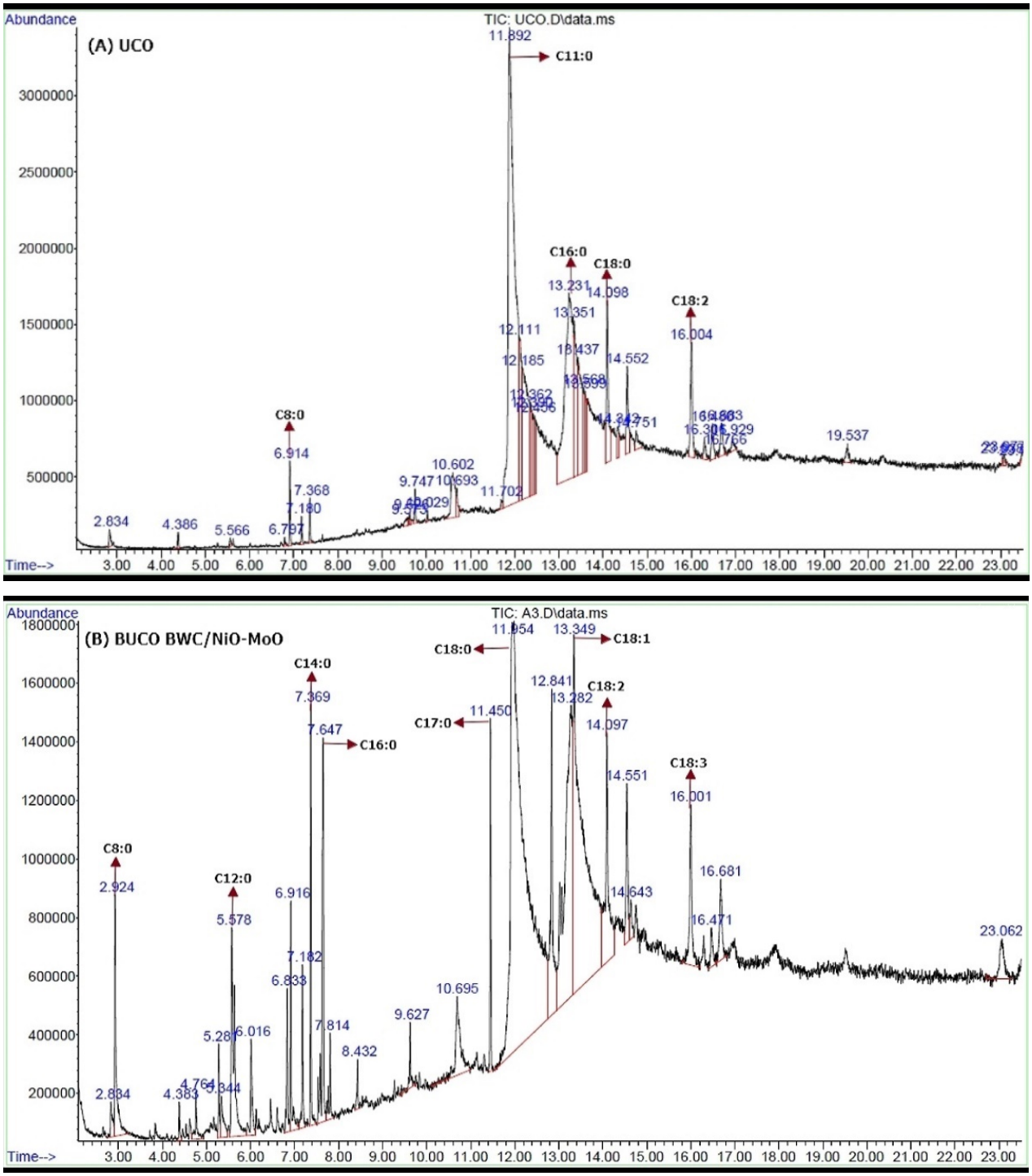


Figure 8. (**A**) Fatty acid profile for UCO, and (**B**) fatty acid profile for biodiesel using BWC/NiO-MoO.

Mainly the primary methyl esters such as Octanoic acid (C8), Hexadecenoic acid, Octadecanoic, Oleic acid (C18), Heptadecanoic (C17), Dodecanoic (C12), Nonanoic (C9) acids, etc. were seen in biodiesel. In a similar study, biodiesel produced from waste cooking oil had compounds such as Hexadecenoic acid (C16:1), Octadecanoic acid (C18:1), and other methyl esters. In that study, the authors reported that waste cooking-oil biodiesel had saturated fatty acids of 30.76% and unsaturated fatty acids of 63.92%, respectively [35]. It is evident that the FAME profile has a significant influence on the biodiesel properties. A higher cetane number for a biodiesel is a result of the presence of saturated fatty acid methyl esters. A higher amount of unsaturated fatty acids increases the cloud point or

pour point value, as well as greater combustion and emission properties [36]. The higher viscosity of biodiesel is due to the presence of polyunsaturated and higher sized saturated fatty acids. An increased presence of saturated fatty acids make the biodiesel more stable, high viscous, and results in a higher cetane number [37]. Less viscous and lower cloud points for biodiesel are needed to produce an economical and viable candidate for next generation fuels.

3. Materials and Methods

3.1. Biochar Supply and Process

Wood chips supplied by Worldwide Landfills were transported to the UPM Biorefinery Complex for carbonization using the UPM technology developed in collaboration with Kyushu Institute of Technology (Kyutech, Japan). The pyrolysis-based method was specifically developed and employed for the synthesis of biochar. The Biomass Microwave Carbonizer (BMC) is a microwave-assisted oxygen-free combustion system. The incineration system takes place in a well-balanced burning chamber at a low temperature (250–300 °C), with a temperature-regulated and adjustable, automated panel. The biochar produced by BMC is different to the normal, incineration process due to its high carbon yield, power rating, time savings, and low emissions.

3.1.1. Feedstock

Used cooking oil (UCO), mainly from palm oil, was collected from food premises around Bintulu Sarawak, Malaysia. The oils were filtered and checked for their acid value and FFA before transesterification.

3.1.2. Chemicals

During the acid pre-treatment of biochar, 85% laboratory grade phosphoric acid (H_3PO_4) was employed. Methanol (CH_3OH) supplied by HmbG Chemicals was utilized during transesterification and titration. Two transition metals were utilized in the impregnation method: (a) nickel (II) nitrate hexahydrate (Ni $(NO_3)_2.6H_2O$) with a molecular weight 290.79 g/mol and (b) ammonium molybdate ($(NH_4)_6Mo_7.4H_2O$) with molecular weight 1235.86 g/mol both supplied by HmbG Chemicals.

3.1.3. Preparation of Catalyst

Biochar Activation under Reflux Acid Pre-Treatment

The biochar was weighed before being placed in a round bottom flask, a respective volume of phosphoric acid then was added, these were mixed together with a magnetic stirrer before connecting the reflux condenser. The hotplate was set with the required temperature, rpm, and time for the reaction. Next, purification was carried out using distilled water before being oven dried overnight. The powder was then impregnated with two metal oxides at a ratio of 10% (NiO): 10% (MoO): 80% (biochar) under continuous stirring for 6 h. Then the mixture was oven dried overnight again at 100 °C before calcination in the furnace for 4 h at 400 °C and 800 °C under nitrogen gas flow.

3.1.4. Catalytic Transesterification of Waste Cooking Oil

The UCO was first pre-treated through filtration (to remove chunks and food waste) and heating (to remove excess moisture) before transesterification under reflux conditions. After pre-treatment, a preliminary analysis of the UCO, specifically testing the FFA value, was conducted (max. 5%). The transesterification process was carried out by hybridizing a synthetic heterogeneous catalyst (5 wt.% oil weight) with a methanol ratio of 1:1 (10:1). Heating occurred at a constant temperature of 65 °C, 75 °C, 85 °C, or 95 °C at a constant RPM of 500. Following the heating process, the mixture was allowed to stand for 1 h or more until visible precipitates of the separation process appeared. The separation process was completed by discharging the bottom liquid first (glycerol), then the waste unreacted methanol, and finally the upper liquid (biodiesel). The removal of impurities, silt, and

grime from the biodiesel was performed by washing it with hot water. Basically, in this experiment, a 3:1 ratio of biodiesel to washing water was sufficient to create a clear biodiesel hue. The moisture was removed from the biodiesel by heating at 100 °C for 30 min with continuous stirring on a hot plate. The European EN 14214, American ASTM D6751, and Malaysian Standard MS 2008 were used in the qualitative examination of biodiesel properties. Equation (1) below describes the yield volume (%) of obtained biodiesel.

$$Biodiesel\ yield\ (\%) = \frac{Weight\ of\ Biodiesel}{\text{Weight of Used Cooking Oil (UCO)}} \times 100 \quad (1)$$

3.2. Acid Value Analysis

The FFA content of UCO was determined by titration with 0.1 M KOH standard solution. A 0.1 M KOH solution was prepared and filled a burette. The solvent solutions of ethanol and diethyl ether were prepared in a ratio of 1:1 v/v inside a conical flask. Next, 3 drops of phenolphthalein were added to the solvent solution as an indicator. UCO was weighed and mixed with the solvent solution. The solvent and fat mixture were stirred with a magnetic stirrer, and the 0.1 M KOH solution was titrated into the mixture. The titration was stopped until the color of the solvent and oil mixture turned from clear to pink for more than 10 s. The amount of the 0.1 M KOH solution needed for the titration was noted and the corresponding acid value and FFA of the UCO were calculated with Equations (2) and (3), as derived from [38]:

$$(\text{Volume of 0.01 M KOH} \times 0.01 \times 56.1)/\text{Mass oil (g)} \quad (2)$$

$$\text{FFA} = \text{Acid value}/2 \quad (3)$$

Each experiment was repeated at least three times to obtain the average calculated value, which was reported in mg KOH/g.

3.3. Catalyst Characterization

3.3.1. X-ray Diffraction (XRD)

Before and after the reaction, XRD was used to determine the dispersion and chemical composition of the fresh and impregnated biochar woodchip catalysts. A Shimadzu diffractometer was used to conduct the XRD analysis (model XRD-6000).

3.3.2. Thermal Gravimetry

TGA analysis carried out with a Simultaneous Thermal Analyzer (STA) 8000 was used to measure the stability of the synthesized catalyst. It was also used to explain how the coke deposited on the spent catalyst were determined. Next, the spent catalyst was heated from 25 to 900 °C at a heating rate of 30 °C/min under 40 mL/min oxygen flow as summarized in Table 2 below.

Table 2. Description of the prepared catalyst name.

Type of Catalyst	Description
SBWC8	Spent biochar woodchip doped with nickel and molybdenum metal calcined in temperature 400 °C
SBWC4	Spent biochar woodchip doped with nickel and molybdenum metal calcined in temperature 800 °C
IBWC8	Biochar woodchip doped with nickel and molybdenum metal calcined in temperature 800 °C
IBWC4	Biochar woodchip doped with nickel and molybdenum metal calcined in temperature 400 °C
TBWC	Treated biochar undergone acid pre-treatment
BWC	Fresh biochar woodchip

3.3.3. Field Emission Scanning Electron Microscopy (FESEM)

A scanning electron microscope (SEM) (SEM TM 3030, Hitachi, Japan) Scanning electron microscopy (SEM, TM3030, HITACHI, Tokyo, Japan) was utilized to study the morphology of fresh biochar woodchip impregnated the Ni-Mo catalyst. The study was carried out with 25,000× and 50,000× magnification and 15 kV of accelerating voltage.

3.4. Biodiesel Characterization

3.4.1. Fourier Transform Infrared (FTIR) Spectroscopy

The chemical functional groups of the triolein (feedstock) and transesterified materials were investigated using FTIR. The absorption bands corresponding to ester, alcohol, carbonyl, glycerides, and carboxylic groups were detected during transesterification. With slight modifications, the chemical characterization analysis was carried out in accordance with the method described in the literature [39]. At a resolution of 4 cm^{-1} in the range of 4000–400 cm^{-1} averaged across 16 scans, the Perkin-Elmer Spectrum One FT-IR Spectrometer was used to evaluate the chemical composition and chemical bonds present in the biodiesel.

3.4.2. Gas Chromatography-Mass Spectrometer (GC-MS)

Identification of the unsaturated hydrocarbon and chemical composition of the feedstock and biodiesel was performed by interpretation of the GC-MS data, characterized by GC-MS (model SHIMADZU QP50550A) and by comparison with the mass spectra of the National Institute of Standards and Testing library and literature data [40]. The GC–MS was equipped with a non-polar DB-5HT column (30 m × 0.32 mm × 0.25 µm) with split less inlet. The analysis was important as it showed that the liquid product could not be assumed to be purely hydrocarbons. The samples were diluted with GC grade n-hexane (purity > 98%) to 100 mg/L. The compound was identified based on a probability match equal to or higher than 95%. The selectivity of the liquid products was determined using Equation (4).

$$X = \frac{Ax}{\Sigma Ay} \times 100\% \quad (4)$$

4. Conclusions and Future Recommendation

The results of this research not only describe the production process of biodiesel from UCO, but also the catalyst and biodiesel characterization. The catalyst that was synthesized from biochar BWC was characterized and successfully impregnated with two types of transition metal.

The characterization of the synthesized catalysts using the XRD, FESEM, and TGA proved that BWC/NiO-MoO800 has better performance and is chemically and physically suitable to be used as a heterogeneous catalyst in the biodiesel production process.

The XRD analysis showed great metal dispersion on the active surface of activated biochar, while the FESEM micrograph identified that the two metals were incorporated nicely onto the biochar surface. The TGA result was directly proportional to the other analysis which found the catalyst calcined in temperature of 800 °C to be more stable and perform better in catalytic transesterification.

The UCO used in this research had a relatively low acid value. This enabled the practice of single step transesterification to produce biodiesel. Meanwhile, the optimum parameters for UCOME or biodiesel production have been determined as 5 wt% (0.5 g) catalyst loading, 1:110 methanol to oil ratio, 65–75−85–95 °C reaction temperature, and 120 min of reaction time for this catalyst (BWC/NiO-MoO400, BWC/NiO-MoO800).

Lastly, the biodiesel obtained was characterized and verified by qualitative analysis using the FTIR and GC-MS equipment. Results showed that the highest biodiesel yield was obtained (74.66%) by using biochar from BWC BWC/NiO-MoO800 using a temperature range of 75 °C to 95 °C, with the catalyst reusability up ≥ to five cycles. These parameters can be reused for at least four cycles of transesterification without UCOME yield falling

below 65%. These parameters will be useful for setting up a small to medium sized biodiesel production process, industrially.

In the future, the synthesized catalyst might be utilized in a pilot-scale production process with a slight modification for solid catalyst storage due to its reusability, being able to be used more than four times. Furthermore, additional catalyst characterization such as using temperature programmed desorption (TPD) must be carried out on the woodchip biochar species to obtain detailed information about the preparation of biochar as a catalyst support incorporated with a transition metal (either single or bimetallic) over various parameters such as methanol to oil ratio, reaction temperature, time reaction, and catalyst loading.

Author Contributions: N.S.A.: technical investigation, data generation, and writing original draft; N.K.: funding acquisition, supervision, writing, and review editing; T.S.M.T.A.: writing, review, and editing; S.S.: writing, review, and editing; M.A.H.: biomass supply, review editing. All authors have read and agreed to the published version of the manuscript.

Funding: This research was funded by the Ministry of Higher Education (MOHE) for the FRGS grant (Ref: FRGS/1/2018/TK05/UPM/02/8) and the Research Management Centre (RMC) of the Universiti Putra Malaysia (UPM-IPB 9671301). Thank you to the Universiti Malaysia Pahang (UMP) for the great and prompt help with facilities and instruments for sample analysis that allowed for the smooth project analysis.

Data Availability Statement: Not applicable.

Acknowledgments: The authors thank the Ministry of Higher Education (MOHE) for the FRGS grant ((Ref: FRGS/1/2018/TK05/UPM/02/8)) and the Research Management Centre (RMC) of Universiti Putra Malaysia (UPM-IPB 9671301) for supporting this study. The highest appreciation also goes to the Department of Science and Technology, Faculty of Humanities, Management and Science, Universiti Putra Malaysia Bintulu Sarawak Campus. The authors also credit the Biorefinery Complex UPM Serdang for the biomass (woodchip biochar) supply. Thank you to the Universiti Malaysia Pahang (UMP) for the great and prompt help with facilities and instruments for sample analysis that allowed for the smooth project analysis.

Conflicts of Interest: The authors declare no conflict of interest.

References

1. Fadhil, A.B.; Saeed, I.K.; Saeed, L.I.; Altamer, M.H. Co-solvent ethanolysis of chicken waste: Optimization of parameters and characterization of biodiesel. *Energy Sources Part A Recovery Util. Environ. Eff.* **2016**, *38*, 2883–2890. [CrossRef]
2. Boulal, A.; Atabani, A.E.; Mohammed, M.N.; Khelafi, M.; Uguz, G.; Shobana, S.; Bokhari, A.; Kumar, G. Integrated valorization of Moringa oleifera and waste Phoenix dactylifera L. dates as potential feedstocks for biofuels production from Algerian Sahara: An experimental perspective. *Biocatal. Agric. Biotechnol.* **2019**, *20*, 101234. [CrossRef]
3. Gai, L.; Varbanov, P.S.; Van Fan, Y.; Klemeš, J.J.; Romanenko, S.V. Trade-offs between the recovery, exergy demand and economy in the recycling of multiple resources. *Resour. Conserv. Recycl.* **2021**, *167*, 105428. [CrossRef]
4. Moayedi, H.; Aghel, B.; Abdullahi, M.M.; Nguyen, H.; Safuan ARashid, A. Applications of rice husk ash as green and sustainable biomass. *J. Clean. Prod.* **2019**, *237*, 117851. [CrossRef]
5. Hamza, M.; Ayoub, M.; Shamsuddin, R.B.; Mukhtar, A.; Saqib, S.; Zahid, I.; Ameen, M.; Ullah, S.; Al-Sehemi, A.G.; Ibrahim, M. A review on the waste biomass derived catalysts for biodiesel production. *Environ. Technol. Innov.* **2021**, *21*, 101200. [CrossRef]
6. Liew, J.X.; Loy, A.C.M.; Chin, B.L.F.; AlNouss, A.; Shahbaz, M.; Al-Ansari, T.; Govindan, R.; Chai, Y.H. Synergistic effects of catalytic co-pyrolysis of corn cob and HDPE waste mixtures using weight average global process model. *Renew. Energy* **2021**, *170*, 948–963. [CrossRef]
7. Hajinezhad, A.; Abedi, S.; Ghobadian, B.; Noorollahi, Y. Biodiesel pro-duction from Norouzak (Salvia lerifolia) seeds as an indigenous source of bio fuel in Iran using ultrasound. *Energy Convers. Manag.* **2015**, *99*, 132–140. [CrossRef]
8. Abdullah; Rahmawati Sianipar, R.N.; Ariyani, D.; Nata, I.F. Conversion of palm oil sludge to biodiesel using alum and KOH as catalysts. *Sustain. Environ. Res.* **2017**, *27*, 291–295. [CrossRef]
9. Semwal, S.; Arora, A.K.; Badoni, R.P.; Tuli, D.K. Biodiesel production using heterogeneous catalysts. *Bioresour. Technol.* **2011**, *102*, 2151–2161. [CrossRef]
10. Balajii, M.; Niju, S. Biochar-derived heterogeneous catalysts for biodiesel production. *Environ. Chem. Lett.* **2019**, *17*, 1447–1469. [CrossRef]
11. Nguyen, H.C.; Nguyen, M.L.; Su, C.H.; Ong, H.C.; Juan, H.Y.; Wu, S.J. Bio-derived catalysts: A current trend of catalysts used in biodiesel production. *Catalysts* **2021**, *11*, 812. [CrossRef]

12. Salomon-Negrete, M.A.; Reynel-Avila, H.E.; Mendoza-Castillo, D.I.; Bonilla-Petriciolet, A.; Duran-Valle, C.J. Water defluoridation with avocado-based ad- sorbents: Synthesis, physicochemical characterization and thermodynamic studies. *J. Mol. Liq.* **2018**, *254*, 188–197. [CrossRef]
13. Merodio-Morales, E.E.; Reynel-Avila, H.E.; Mendoza-Castillo, D.I.; Duran-Valle, C.J.; Bonilla-Petriciolet, A. Lanthanum- and cerium-based functionalization of chars and activated carbons for the adsorption of fluoride and arsenic ions. *Int. J. Environ. Sci. Technol.* **2020**, *17*, 115–128. [CrossRef]
14. Arun, N.; Sharma, R.V.; Dalai, A.K. Green diesel synthesis by hydrode-oxygenation of bio-based feedstocks: Strategies for catalyst design and develop-ment. *Renew. Sustain. Energy Rev.* **2015**, *48*, 240–255. [CrossRef]
15. Kim, J.; Yoo, G.; Lee, H.; Lim, J.; Kim, K.; Kim, C.W.; Park, M.S.; Yang, J.W. Methods of downstream processing for the production of biodiesel from microalgae. *Biotechnol. Adv.* **2013**, *31*, 862–876. [CrossRef] [PubMed]
16. Festel, G.; Würmseher, M.; Rammer, C.; Boles, E.; Bellof, M. Modelling production cost scenarios for biofuels and fossil fuels in Europe. *J. Clean. Prod.* **2014**, *66*, 242–253. [CrossRef]
17. Rezania, S.; Kamboh, M.A.; Arian, S.S.; Al-Dhabi, N.A.; Arasu, M.V.; Esmail, G.A.; Kumar Yadav, K. Conversion of waste frying oil into biodiesel using recoverable nanocatalyst based on magnetic graphene oxide supported ternary mixed metal oxide nanoparticles. *Bioresour. Technol.* **2021**, *323*, 124561. [CrossRef]
18. Azman, N.S.; Marliza, T.S.; Asikin-Mijan, N.; Hin TY, Y.; Khairuddin, N. Production of biodiesel from waste cooking oil via deoxygenation using ni-mo/ac catalyst. *Processes* **2021**, *9*, 750. [CrossRef]
19. Fadhil, A.B.; Aziz, A.M.; Altamer, M.H. Potassium acetate supported on activated carbon for transesterification of new non-edible oil, bitter almond oil. *Fuel* **2016**, *170*, 130–140. [CrossRef]
20. Alaei, S.; Haghighi, M.; Toghiani, J.; Rahmani Vahid, B. Magnetic and reusable $MgO/MgFe_2O_4$ nanocatalyst for biodiesel production from sunflower oil: Influence of fuel ratio in combustion synthesis on catalytic properties and performance. *Ind. Crops Prod.* **2018**, *117*, 322–332. [CrossRef]
21. Hanif, M.A.; Nisar, S.; Akhtar, M.N.; Nisar, N.; Rashid, N. Optimized production and advanced assessment of biodiesel: A review. *Int. J. Energy Res.* **2018**, *42*, 2070–2083. [CrossRef]
22. Kostić, M.D.; Djalović, I.G.; Stamenković, O.S.; Mitrović, P.M.; Adamović, D.S.; Kulina, M.K.; Veljković, V. Kinetic modeling and optimization of biodiesel production from white mustard (*Sinapis alba* L.) seed oil by quicklime-catalyzed transesterification. *Fuel* **2018**, *223*, 125–139. [CrossRef]
23. Mercy Nisha Pauline, J.; Sivaramakrishnan, R.; Pugazhendhi, A.; Anbarasan, T.; Achary, A. Transesterification kinetics of waste cooking oil and its diesel engine performance. *Fuel* **2021**, *285*, 119108. [CrossRef]
24. Odetoye, T.E.; Agu, J.O.; Ajala, E.O. Biodiesel production from poultry wastes: Waste chicken fat and eggshell. *J. Environ. Chem. Eng.* **2021**, *9*, 105654. [CrossRef]
25. Mazaheri, H.; Ong, H.C.; Masjuki, H.H.; Amini, Z.; Harrison, M.D.; Wang, C.T.; Kusumo, F.; Alwi, A. Rice bran oil based biodiesel production using cal-cium oxide catalyst derived from Chicoreus brunneus shell. *Energy* **2018**, *144*, 10–19. [CrossRef]
26. Syazwani, O.N.; Teo, S.H.; Islam, A.; Taufiq-Yap, Y.H. Transesterifica-tion activity and characterization of natural CaO derived from waste venus clam (*Tapes belcheri* S.) material for enhancement of biodiesel production. *Process Saf. Environ. Prot.* **2017**, *105*, 303–315. [CrossRef]
27. Li, M.; Zheng, Y.; Chen, Y.; Zhu, X. Biodiesel production from waste cooking oil using a heterogeneous catalyst from pyrolyzed rice husk. *Bioresour. Technol.* **2014**, *154*, 345–348. [CrossRef]
28. Yang, H.; Yan, R.; Chen, H.; Lee, D.H.; Zheng, C. Characteristics of hemicellulose, cellulose and lignin pyrolysis. *Fuel* **2007**, *86*, 1781–1788. [CrossRef]
29. Lee, J.; Kim, K.H.; Kwon, E.E. Biochar as a Catalyst. *Renew. Sustain. Energy Rev.* **2017**, *77*, 70–79. [CrossRef]
30. Yu, J.T.; Dehkhoda, A.M.; Ellis, N. Development of biochar-based cata-lyst for transesterification of canola oil. *Energy Fuels* **2011**, *25*, 337–344. [CrossRef]
31. Niju, S.; Kirthikaa, M.; Arrthi, S.; Dharani, P.; Ramya, S.; Balajii, M. Fish-Bone-Doped Sea Shell for Biodiesel Production from Waste Cooking Oil. *J. Inst. Eng. Ser. E* **2020**, *101*, 53–60. [CrossRef]
32. Abdulkareem-Alsultan, G.; Asikin-Mijan, N.; Lee, H.V.; Taufiq-Yap, Y.H. A new route for the synthesis of La-Ca oxide supported on nano activated carbon via vacuum impregnation method for one pot esterification-transesterification re-action. *Chem. Eng. J.* **2016**, *304*, 61–71. [CrossRef]
33. Goswami, L.; Kushwaha, A.; Singh, A.; Saha, P.; Choi, Y.; Maharana, M.; Patil, S.V.; Kim, B.S. Nano-Biochar as a Sustainable Catalyst for Anaerobic Diges-tion: A Synergetic Closed-Loop Approach. *Catalysts* **2022**, *12*, 186. [CrossRef]
34. Hanafi, S.A.; Elmelawy, M.S.; Shalaby, N.H.; El-Syed, H.A.; Eshaq, G.; Mostafa, M.S. Hydrocracking of waste chicken fat as a cost effective feedstock for re-newable fuel production: A kinetic study. *Egypt. J. Pet.* **2016**, *25*, 531–537. [CrossRef]
35. Ganesan, R.; Manigandan, S.; Shanmugam, S.; Chandramohan, V.P.; Sindhu, R.; Kim, S.H.; Brindhadevi, K.; Pugazhendhi, A. A detailed scrutinize on panorama of catalysts in biodiesel synthesis. *Sci. Total Environ.* **2021**, *777*, 145683. [CrossRef]
36. Altun, Ş. Effect of the degree of unsaturation of biodiesel fuels on the exhaust emissions of a diesel power generator. *Fuel* **2014**, *117 Pt A*, 450–457. [CrossRef]
37. Murugesan, A.; Subramaniam, D.; Avinash, A.; Nedunchezhian, N. Quantitative and qualitative analysis of biodiesel—An in-depth study. *Int. J. Ambient. Energy* **2015**, *36*, 19–30. [CrossRef]

38. Anastopoulos, G.; Zannikou, Y.; Stournas, S.; Kalligeros, S. Transesterification of vegetable oils with ethanol and characterization of the key fuel properties of ethyl esters. *Energies* **2009**, *2*, 362–376. [CrossRef]
39. Muhammad, N.; Man, Z.; Bustam, M.A.; Mutalib MI, A.; Rafiq, S. Investigations of novel nitrile-based ionic liquids as pretreatment solvent for extraction of lignin from bamboo biomass. *J. Ind. Eng. Chem.* **2013**, *19*, 207–214. [CrossRef]
40. Asomaning, J.; Mussone, P.; Bressler, D.C. Thermal deoxygenation and pyrolysis of oleic acid. *J. Anal. Appl. Pyrolysis* **2014**, *105*, 1–7. [CrossRef]

Disclaimer/Publisher's Note: The statements, opinions and data contained in all publications are solely those of the individual author(s) and contributor(s) and not of MDPI and/or the editor(s). MDPI and/or the editor(s) disclaim responsibility for any injury to people or property resulting from any ideas, methods, instructions or products referred to in the content.